NMR IN BIOMEDICINE
NMR Biomed. 2006; **19**: 723–730
Published online in Wiley InterScience
(www.interscience.wiley.com) DOI:10.1002/nbm.1101

Advances in MR imaging of the skin†

Jacques Bittoun,[1]* Bernard Querleux[2] and Luc Darrasse[1]

[1]U2R2M, CNRS-Université Paris-Sud, CIERM Hôpital Bicêtre, 94275 Le Kremlin-Bicêtre, France
[2]L'Oréal Recherche, Aulnay-sous-Bois, France

Received 30 January 2006; Revised 28 July 2006; Accepted 9 August 2006

ABSTRACT: MR imaging of the skin is challenging because of the small size of the structures to be visualized. By increasing the gradient amplitude and/or duration, skin layers can be visualized with a voxel size of the order of 20 μm, clearly the smallest obtained for *in vivo* images in a whole-body imager. Currently, the gradient strength of most commercial systems enables acquisition of such a small voxel size, and the main difficulty has thus become to achieve sufficient detection sensitivity. The signal-to-noise ratio (SNR) can be increased either by increasing the magnetic field strength or by minimizing noise with small coils; cooling copper coils or superconducting coils can enhance the SNR by a factor of 3 or more. MR imaging, because of the large number of parameters it is able to measure, can provide more than the microscopic architecture of the skin: physical parameters such as relaxation times, magnetization transfer or diffusion, and chemical parameters such as the water and fat contents or phosphorus metabolism. In spite of the amount of information they have provided to date, MR imaging and spectroscopy have had limited clinical applications, mainly because cutaneous pathologies are easily accessible to the naked eye and surgery. However, MR technologies indeed represent powerful research tools to study normal and diseased skin. Copyright © 2006 John Wiley & Sons, Ltd.

KEYWORDS: chemical-shift imaging; diffusion imaging; high-resolution MR imaging; magnetization transfer; skin imaging; superconductive coils

INTRODUCTION

The skin can easily be directly examined with the eyes, and most pathologies can be diagnosed without recourse to imaging methods. However, many particular aspects of the skin are better evaluated by non-invasive imaging methods. First is its morphology, as skin is composed of many superimposed layers, with different characteristics, properties and functions, that cannot be differentiated by the naked eye but are clearly delineated by imaging methods. In addition, most functions involve microscopic structures, such as hair follicles and sebaceous glands that are not visible to the naked eye. Finally, regardless of its resolution power, the eye can only see superficial anatomy, whereas imaging methods can provide information on skin physiology and physiopathology.

Among the available techniques, MR imaging does not give the highest spatial resolution but it provides excellent information on anatomy and physical and chemical tissue parameters. Advances made in imaging technologies by many research teams throughout the world continue to improve skin MR imaging. In this paper the field of skin MR imaging for anatomical and physicochemical characterization of the skin is reviewed. Potential clinical applications are also discussed. For each section, a brief summary of well-established results is provided from a historical perspective for the newcomer by highlighting the challenges posed by very high-resolution MR imaging of the skin.

**Correspondence to:* J. Bittoun, CIERM-Hôpital Bicetre, 78, rue du Général Leclerc, 94275 Le Kremlin-Bicêtre, France.
E-mail: jacques.bittoun@cierm.u-psud.fr

Abbreviations used: ADC, apparent diffusion coefficient; CNR, contrast-to-noise ratio; HTS, high-temperature superconductor; MR, magnetic resonance; MT, magnetization transfer; RF, radiofrequency; SNR, signal-to-noise ratio.

†This paper is published as part of a Special Issue entitled "NMR of the Musculoskeletal System."

SPATIAL RESOLUTION AND SKIN ANATOMY

The skin is composed of four main layers (Fig. 1): the stratum corneum, the outermost protective layer, mainly composed of dead keratinocytes; the epidermis, the layer of active multiplication and differentiation of keratinocytes, among other functions; the dermis: fibrous tissue rich in collagen, further subdivided into the papillary dermis and the reticular dermis, which contains cutaneous appendages, such as sebaceous glands and the larger part of pilosebaceous units; and the hypodermis or fat tissue which is sometimes considered part of the skin and sometimes as subcutaneous tissue.

The thickness of these layers varies according to anatomic area, but the order of magnitude is centimetres for the hypodermis, millimetres for the dermis and 100 μm for the epidermis and stratum corneum. Hence, the minimum depth resolution required to separate the

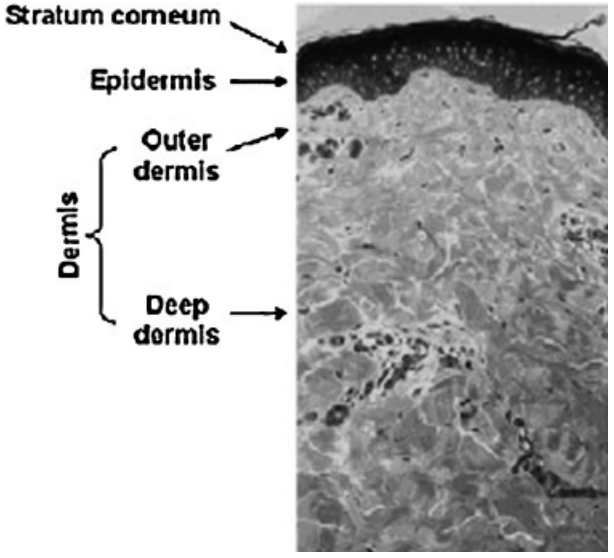

Figure 1. Histological section of normal skin without hypodermis, showing the layered structure to be visualized by MR imaging

skin layers is 100 μm. Paradoxically, such resolution in a whole-body magnet was reached for the first time at 0.1 T, a magnetic field strength already considered low in 1988 (1). Querleux *et al.* (1) introduced the notion of the surface-gradient insert and the small copper-loop surface coil. The gradient insert, required to reduce the voxel size, could only generate a magnetic field gradient perpendicular to the skin. This apparent drawback was turned into an advantage by acquiring anisotropic voxels. Because the signal-to-noise ratio (SNR) is proportional to the voxel volume, such anisotropy of the acquisition is often chosen in MR skin imaging, as it allows clear delineation of the skin layers without excessive diminution of the voxel volume. The direction of the strongest gradient was chosen as the frequency-encoding direction. The voxel size in this direction is given by

$$\delta x = \frac{1}{\frac{\gamma}{2\pi} G_{\text{freq}} \cdot t_{\text{O}}} \qquad (1)$$

in which $\gamma/2\pi$ represents the gyromagnetic ratio equal to 42.58 MHz/T for the proton. This simple equation shows that the voxel size is inversely proportional to the gradient amplitude in the frequency-encoding direction, G_{freq}, and to the time of observation (i.e. sampling) of each signal, t_{O}. The small size of the gradient coil enabled a gradient amplitude of up to 85 mT/m at a time when the maximum gradient amplitude of most commercial systems was about 10 mT/m.

The role of the small surface coil was to compensate for the SNR loss resulting from the small voxel size. The reduction in the sensitive volume of the coil was a way to filter out the noise from the rest of the sample: owing to its random nature, noise is not localized, so that each pixel of the image contains the signal of the corresponding voxel and the noise originating from the whole volume detected by the coil. More quantitatively, the reciprocity theorem states that the electromotive force detected in the coil windings is proportional to the magnetic coupling factor B_1/I, i.e. the magnetic field B_1 produced in a given voxel per unit radiofrequency (RF) current I supplied to the coil. The SNR delivered by the coil is then given as a function of the voxel volume v_0 and the transverse magnetization M_{T} available over the observation time t_{O} (2):

$$\text{SNR} \propto \frac{B_1/I}{\sqrt{R_{\text{S}}T_{\text{S}} + R_{\text{C}}T_{\text{C}}}} v_0 \, M_{\text{T}} \, \sqrt{t_{\text{O}}} \qquad (2)$$

where the equivalent loss resistances R_{S} and R_{C} and temperatures T_{S} and T_{C} represent the random noise contributed by the sample and coil respectively. Decreasing the surface coil diameter linearly increases B_1/I at close proximity to the coil, while the sample resistance R_{S} (and hence noise power) increases as the diameter to the third power. Thus, coil size reduction provides a very efficient way locally to improve the SNR by scaling the reciprocal of the diameter up to the power of 5/2, as long as the coil resistance R_{C} can be kept sufficiently small. The logical consequence is that the sensitivity of any coil should be confined to the volume of interest, which, for skin MR imaging, corresponds at most to the first centimetre below the body surface.

The gradient and RF coils were incorporated into a skin-imaging module, which was subsequently transferred to a 1.5 T whole-body MR system, thereby increasing the net magnetization per unit volume and enabling acquisitions of smaller voxel size. With this system, images of normal skin in most anatomic regions could be obtained with highly anisotropic voxels of $70 \times 390 \times 3000\ \mu\text{m}^3$, with the smallest dimension being perpendicular to the skin surface in order better to delineate the different skin layers (3) (Fig. 2).

The requirement of a custom-built add-on module to obtain MR images of the skin severely limited the use of skin imaging. As shown by eqn (1), the voxel size can also

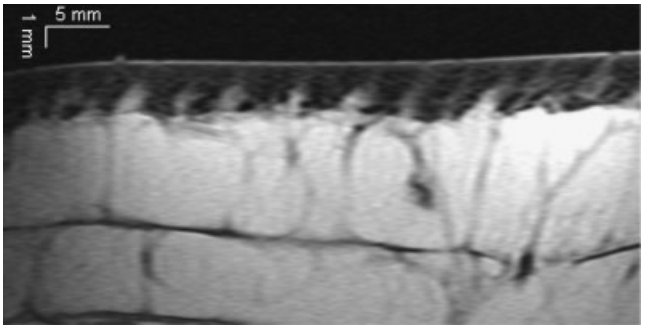

Figure 2. Image of normal thigh skin obtained with a dedicated MR skin-imaging module. The anisotropy of the voxel ($70 \times 390 \times 3000\ \mu\text{m}^3$) enabled high resolution perpendicular to the skin surface while maintaining a sufficient SNR. The image shows dermis appendages that can be further analysed by MR spectroscopy (see Fig. 5)

DOI: 10.1002/nbm

be reduced by increasing the time of observation of each signal. Thus, by increasing t_O, images of the skin could be obtained with a gradient amplitude of 23 mT/m (4,5), an amplitude easily reached with the standard gradient coils available in the 1990s. Since increasing t_O corresponds to simultaneously decreasing the image frequency bandwidth, this method has the additional advantage of increasing SNR. By using a very small square ($1 \times 1\,cm^2$) surface coil and a reduced bandwidth, Song *et al*. obtained images of calf skin in a few minutes with a voxel volume as small as $19 \times 78 \times 800\,\mu m^3$(5).

Currently, with gradient amplitude reaching and even exceeding 40 mT/m in most commercial MR systems, decreasing the voxel size in the three spatial dimensions is no longer a problem. However, spatial resolution is equal to the voxel size only at a high contrast-to-noise ratio (CNR). Because the CNR is proportional to the voxel volume, decreasing the voxel size implies a CNR reduction at the cost of spatial resolution. Thus, the sensitivity of detection becomes the main limit to spatial resolution. Anisotropic voxel size is the simplest solution to improve the depth resolution by sacrificing resolution in the two dimensions of the skin surface. Pushing this solution to its limit, McDonald *et al*. (6) proposed the use of GARField (Gradient At Right angles to Field) magnets: bench-top permanent magnets with curved pole pieces that create a very strong static magnetic field gradient. With such a system, they succeeded in achieving a resolution of 5–10 μm in a direction perpendicular to the skin, with a magnetic field strength of 0.7 T and a gradient amplitude equal to 17.5 T/m. However, that system does not give real images but rather skin profiles, enabling analysis of skin layers without showing their structure.

To decrease the voxel size in more than one direction, SNR must be increased in some way. One solution consists in increasing the magnetic field strength, thus increasing proportionally the net magnetization and hence the signal from each voxel. Images with an isotropic resolution of about 50 μm in each direction, once obtained with skin samples in high magnetic field MR microscopes (7), could be feasible *in vivo* with the most recent 9.4 T or higher whole-body MR imagers. However, this solution would limit the use of MR skin imaging to the few labs owning such research systems.

An alternative way to increase the SNR without requiring very strong fields is further to reduce the surface coil diameter and lower temperature drastically. The surface coil must be cooled when the sensitive volume is so small that the noise originating from the body becomes less than the noise from the coil material. At 1.5 T, this situation occurs with copper coils at diameters below 3 cm or when a smaller part of the body, such as the finger, is explored. An SNR gain of about 2.7 could be obtained on images of the finger with a voxel size of $78 \times 78 \times 1000\,\mu m^3$ by simply cooling a 2 cm diameter copper coil down to 77 K, the temperature of a liquid nitrogen bath (8), as compared with the same coil at room temperature. For even smaller coils, a still higher gain can be obtained by using a high-temperature superconducting (HTS) material instead of copper (9) to comply with the condition of the diameter to the power of 5/2 mentioned above. Using a 12 mm diameter, flat HTS resonator cooled to 80 K, Ginefri *et al*. (10) increased the SNR by a factor of 3.2 for calf skin, compared with that obtained with a copper coil of same dimension at room temperature. The resonator was made of a thin YBaCuO (yttrium–barium–copper oxide) film etched on both sides of a monocrystalline dielectric substrate. The coil exhibited an unloaded quality factor of 11 000 owing to its extremely low equivalent resistance R_C. With a dedicated cryostat allowing a coil sample separation of 1 mm, including thermal insulation vacuum, the coil quality factor dropped down to 1100 when applied against the calf. For comparison, the quality factor of the equivalent room-temperature copper coil remained at about 100, with only a few percentage points separating loaded and unloaded conditions.

Figure 3 shows an image of the calf skin with a voxel volume of $40 \times 80 \times 900\,\mu m^3$ obtained with such an HTS

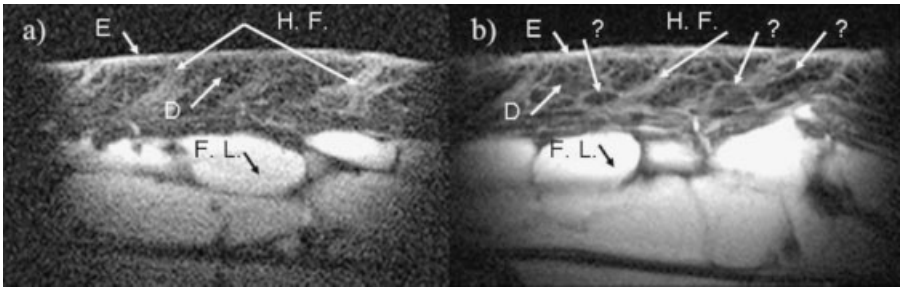

Figure 3. *In vivo* images of calf skin of a normal volunteer obtained using a 1.5 T body scanner (GE, SIGNA) (a) with room-temperature copper or (b) HTS surface coils of the same average diameter of 12 mm. Acquisition was done with a standard 2D spin-echo sequence (*TR*/*TE* = 600/21 ms) on a 512×256 matrix with 39 μm (vertical) by 78 μm (horizontal) voxel size and a slice thickness of 900 μm, a sampling time t_O of 41 ms and a total scan time of 10 min. The following structures can be recognized: E, epidermis; D, dermis; F.L., fat lobule; H.F., hair follicle. Question marks represent unassigned structures

DOI: 10.1002/nbm

coil, and the corresponding image obtained with the equivalent room-temperature copper coil. The HTS coil image clearly delineates not only the different skin layers and pilosebaceous units in the dermis but also very thin fibrillar structures which remain to be assigned (probably a network of vessels containing liquid owing to their high signal intensity), not seen on the image acquired with the copper coil. The detail seen on the HTS images suggests that the CNR is sufficiently high to achieve spatial resolution equal to a voxel volume of less than 3/1000 mm^3. Although such a volume still contains many hundreds of cells, it already represents an *in vivo* histological visualization of the skin structure. The next challenge consists in measuring multiple parameters in such small voxels in order to characterize the skin tissues.

CHARACTERIZATION OF THE SKIN

The great potential of MR medical applications is largely due to the capacity of this technology locally to measure numerous parameters. Some of them represent the physical tissue characteristics, others give information on the chemical composition of tissues. These two categories also exist in skin MR imaging. The difference here again is that the localization of measurements must be much more precise than for any other organ, because of the small area being examined.

Physical parameters

As for any other tissue, the skin signal on standard proton MR images originates from water and lipid molecules, with the signals from other molecules being negligible. However, owing to its close proximity to macromolecules, skin water is unique in many aspects that influence the three main contrast parameters: proton density N(H), longitudinal relaxation time T_1 and transverse relaxation time T_2. Using the skin-imaging module at 1.5 T, Richard *et al*. (11) measured a T_1 in the epidermis and dermis of about 900 ms, whereas T_2 was between 13 and 23 ms. Such a large ratio between T_1 and T_2 is compatible with the major contribution of bound protons characterized by very long T_1 and very short T_2. The same authors also measured these parameters in ageing skin, showing that only proton density in the outer dermis tended to increase, in good agreement with the known decrease in macromolecular content of older peoples' skin (12). By using much shorter echo times (*TE*), Song *et al*. (5) could fit the signal decay to a biexponential curve showing 91% of the dermis proton signal to have a T_2 value less than 10 ms, corresponding to water molecules closely associated with macromolecules, whereas the remaining signal with a T_2 of 42.7 ms was interpreted as belonging to water less tightly bound to collagen. The same authors proposed an acquisition sequence based on variable *TE* in order to shorten the echo time, thereby enhancing protons of the fast-decaying components (13).

Water mobility can also be quantified by magnetization transfer (MT) contrast. Since water tightly bound to protons has a very short T_2 and hence a very large spectral line width, it can be specifically excited either by off-resonance or binomial pulses. Although their signal would be too short to contribute to contrast, the saturation caused by their selective excitation can be transferred to mobile protons whose signal will subsequently be decreased in the image (14). The MT can be quantified by the signal amplitude decrease when exciting the bound protons before image acquisition. Mirrashed and Sharp (15) were able to measure MT activity in skin layers (defined by the authors as the expression $[(1-M_S/M_0) \times 100]$, where M_0 is the equilibrium magnetization and M_s is the magnetization measured in MT images). They showed that the stratum corneum could be better delineated by MT activity, which was lower in the stratum corneum. They could also distinguish two dermis layers corresponding to the papillary dermis and reticular dermis, with the latter having lower MT activity.

The mobility of free water can itself be evaluated by the water diffusion coefficient. Kinsey *et al*. (7) measured the apparent diffusion coefficient (ADC) of *in vitro* preparations of hydrated rat skin in a 600 MHz wide-bore spectrometer equipped with actively shielded imaging gradients. The ADC was $8.6 \pm 2.9 \times 10^{-6}\,cm^2/s$ in the lower epidermis. Owing to low signal intensity, the ADC of the dermis could not be measured, but the authors found that the ADC in hair follicles decreased with age, from $8.2 \pm 2.6 \times 10^{-6}\,cm^2/s$ in the younger skin to $7.6 \pm 2.3 \times 10^{-6}\,cm^2/s$ in the older skin. Lee *et al*. (16) measured an ADC of about $1.35 \times 10^{-5}\,cm^2/s$ in normal skin samples excised from Guinea pigs. They also showed that the ADC increased by more than a factor 2 after exposure to UVB radiation. More recently, using the GARField magnet method, McDonald *et al*. (6) measured an ADC of about $8.5 \times 10^{-6}\,cm^2/s$ at the level of the epidermis on profiles of *in vivo* human skin.

The authors of this review recently conducted preliminary studies of 2D diffusion-weighted MR imaging to explore the water mobility in living epidermis and dermis. Age-related effects were evaluated by comparing two groups of healthy volunteers: ten young women (25 ± 3 years) and ten older women (65 ± 3 years). In the epidermis, the ADC was measured in the two pixels (70 μm = 2 × skin depth pixel size of 35 μm) with the highest values obtained from the mean signal intensity profile in skin depth with a slice thickness of 6 mm. In the outer part of the dermis, the ADC value was calculated from three rectangular regions of interest about 105 μm thick, located below the living epidermis. Finally, the ADC value in the inner dermis was calculated from mean signal intensity values measured in a series of at

DOI: 10.1002/nbm

Table 1. Apparent diffusion coefficient (mean ± SD) of the different skin layers according to age

ADC (10^{-5} cm^2/s)	Young subjects	Aged subjects	Significance of the difference ($p < 0.05$)
Epidermis	2.81 ± 0.25	3.17 ± 0.26	$p = 0.02$
Outer dermis[a]	2.33 ± 0.29	2.85 ± 0.34	$p = 0.006$
Inner dermis	0.90 ± 0.65	1.40 ± 0.60	NS[b]

[a]Outer dermis corresponds to a subepidermal layer about 200 μm thick.
[b]NS = not significant.

least ten isolated pixels to avoid contributions from hypodermal inclusions.

Mean values and standard deviations of the ADC in the skin of young and aged subjects are given in Table 1. These ADC values are probably overestimated, compared with those in other publications, owing to difficulties in calibrating the gradient amplitude applied with the dedicated high-resolution imaging module. However, the present work clearly shows that the ADC values in the direction perpendicular to the skin surface in the epidermis and outer dermis are quite similar while the ADC value in the inner dermis is much lower. If the epidermis and outer dermis are rather isotropic tissues, the inner dermis is much more anisotropic, with the predominant direction of collagen fibres being parallel to the skin surface (17,18), thereby implying restricted diffusion in the direction perpendicular to the skin in accordance with the present measurements.

These findings confirm alterations in the outer part of the dermis, with a statistically significant increase in ADC values perpendicular to the skin surface in older subjects ($p < 0.01$). This increase is in agreement with the results of a previous study that showed more free water N(H) in the outer dermis of older people (12), as well as the known characteristics of skin ageing. The most striking observation was the detection by MR imaging of enhanced water mobility in aged compared with young epidermis. MR diffusion appears to be a very sensitive marker of water mobility in tissues. This finding suggests that the ADC is more sensitive to skin ageing than T_1, T_2 and N(H) which did not show any differences between young and old epidermis with either a voxel size of 70 μm in the previous study (12) or a voxel size of 35 μm in the present study. A similar ADC increase was found in edematous skin (Fig. 4). Measuring water diffusion in living epidermis should contribute to furthering knowledge of the skin barrier-function mechanisms in healthy and diseased skin.

Chemical parameters

As in most soft tissues, the main component of skin is water. However, the skin is special in that it is directly subjected to evaporation and hydration. For this reason, skin hydration and its variations are the target of considerable research interest. Using the high-resolution module, the variation in N(H) in the thick stratum corneum of the heel has been studied in the authors' laboratory under different conditions (19): water bath, application of a moisturizer, repeated soaping. N(H) was found to vary according to the conditions only in the most superficial 400 μm, and never reached the epidermis or dermis. Franconi *et al.* studied the effects of a moisturizing cream applied to the wrists of 15 volunteers (19) and found that T_2 increased 15% in the epidermis after cream application. However, T_2 represents an indirect assessment of hydration and is also a parameter difficult to quantify precisely. The most complete study has been published by Mirrashed and Sharp (20) who associated signal intensity and MT measurements after hydration of the finger-pad skin by water loading and also by applying Vaseline as a barrier to evaporation. They showed that, in the stratum corneum, MT activity increased from 70 to 85%, suggesting that the added water is not free but probably associated with macromolecules. They observed no variation in the epidermis, but found paradoxical decreases in signal intensity and MT activity in the reticular dermis, the deeper layer of dermis. To explain this apparent 'dehydration' of the reticular dermis, which remains to be further studied, the authors proposed structural modifications of the dermis resulting from the stretching of the stratum corneum.

As stated above, fat protons are the second source of signals on MR images. Although spectra of skin lipids contain more than one peak, MR imaging enables dual imaging and/or quantification of protons resonating at the

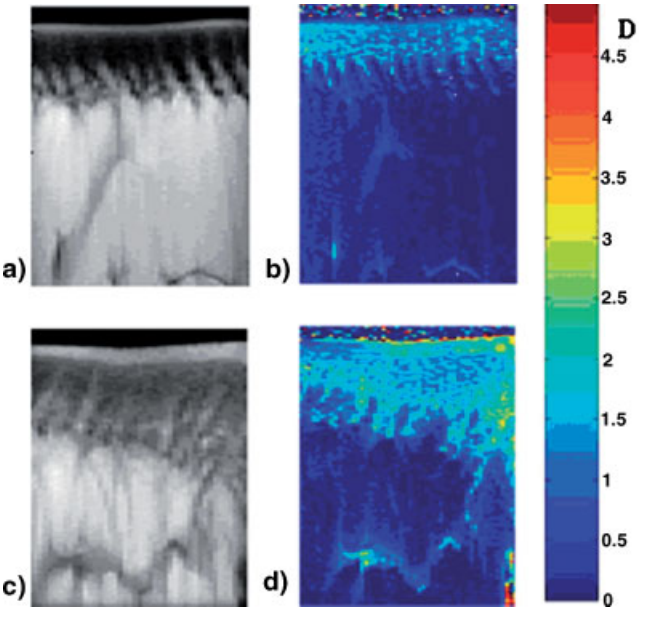

Figure 4. Morphological (a, c) and ADC (b, d) images of normal (a, b) and edematous (c, d) skin. *D* is given in 10^{-5} cm^2/s. The voxel size is 35×625 μm^2 and the slice thickness is 6 mm

DOI: 10.1002/nbm

frequency of water and those resonating at the frequency of CH_2/CH_3 radicals in lipids (which differ by about 140 Hz in a 1 T magnetic field). This separation can be achieved in thin slices of about 300 μm selected in the different layers (21) or by spatial phase encoding in a direction perpendicular to the skin, as described by Wright *et al.* with a spatial resolution of 78 μm (22). Chemical information can also be phase encoded by increasing echo times to produce separate images corresponding to the different resonance frequencies (23). Regardless of the method used, localized proton spectroscopy of the skin enables a better characterization of skin structures, showing, for example, that the lower part of dermis appendages is made of fat while the upper part, in contact with the epidermis, is composed of water (Fig. 5). The acquisition of MR spectra in the hypodermis also enabled analysis of its fat content (24).

While localized proton spectroscopy gives physicochemical information about skin, phosphorus spectroscopy could provide information on skin metabolism. The main difficulty in obtaining *in vivo* ^{31}P spectra of the skin is the need for perfect isolation of the skin because adjacent muscle represents a large reservoir of phosphorus. Most studies published have used a surface coil with restricted depth sensitivity to avoid signal contamination from muscle (25–28). Such a selection method alone (25) is probably insufficient because even minor contamination by muscle in the selected region introduces significant errors. A method based on the acquisition of two spectra at different RF power settings enabled Bohning *et al.* (26) to subtract the contribution of muscle from spectra of the skin and to obtain skin phosphorus spectra of the calves of volunteers: the acquisition time, however, was 4 h and the SNR was 2–3. Using both a depth-selective surface coil 12 mm in diameter and a phase-encoding method generating 0.5 mm thick slices parallel to the skin surface, the present authors' group was unable to detect significant phosphorus signals out of the noise, with acquisition times of the order of 1 h even with a dedicated HTS ^{31}P surface coil with a loaded quality factor of several thousand. However, the detection of phosphorus compounds by spectroscopy of isolated perfused viable epidermal sheets from pigs (29) suggests that, by increasing the acquisition time and/or the sensitive surface of an HTS surface coil, it should be possible to measure precisely localized phosphorus spectra of *in vivo* skin and thus explore skin physiology in normal and pathological conditions.

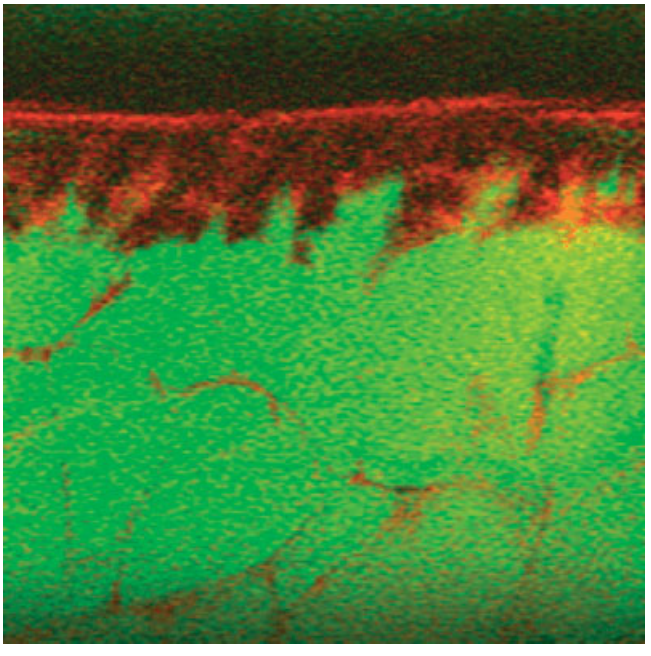

Figure 5. MR spectroscopy image of calf skin with a voxel size of $70 \times 390\ \mu m^2$ and a slice thickness of 3 mm, showing the distribution of signals from water (red) and fat (green) protons. The dermis appendages are clearly separated into an upper part, mainly composed of water, and a lower part, the signal of which reflects the predominance of fat protons

CLINICAL APPLICATIONS

The remarkable anatomic detail obtained on MR images has been used to generate *in vivo* 3D representations of skin pathologies, such as nevi (Fig. 6), acne, psoriasis, etc. (30). Of course, such images are not required for the diagnosis of these pathologies.

Skin-imaging methods have been proposed as a means to estimate the extent of skin tumours before surgery. The aim of most clinical applications of MR imaging of the skin has been to differentiate among the different kinds of skin tumour. Melanomas and pigmented tumours were first explored owing to their high signal intensity on T_1-weighted images (31,32). However, the study on gadolinium uptake failed to distinguish between benign and malignant tumors (33,34). Perhaps the more recent demonstration of a systematic perfusion heterogeneity in melanomas (35,36) provides some elements of an explanation.

With increasing spatial resolution, MR imaging of the skin might hopefully be able to determine the extent of a skin tumour before surgery. Although it is well established that MR obtains a better characterization of tumours, its current spatial resolution is still poorer than that of ultrasound imaging (37). Moreover, the therapeutic strategy of skin tumour excision consists of histological examination of the surgical flap, during the intervention, to guide the excision until tissue becomes free of tumour cells. Presurgical determination of the precise tumour extent can thus be useful only in areas where the size of the excision should be as limited as possible, such as for the face. However, in such regions, the difficulty to reach areas around the nose, mouth or

DOI: 10.1002/nbm

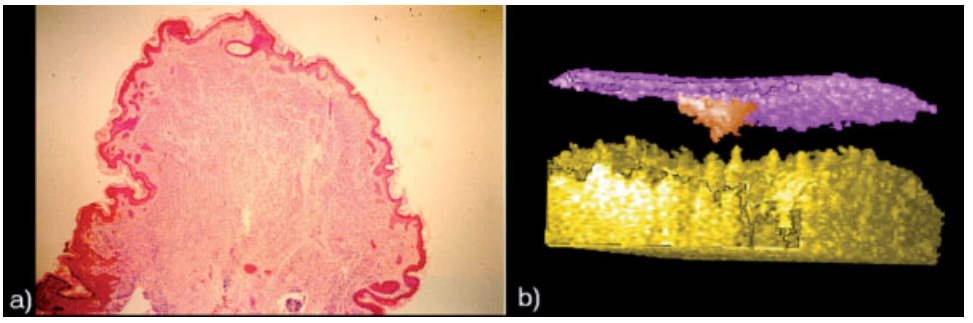

Figure 6. (a) Histological section and (b) 3D-reconstructed MR image of a nevus (voxel volume $70 \times 390 \times 500\ \mu m^3$). The dermis signal was removed by segmentation, enabling precise delineation of the nevus volume (red) between epidermis (purple) and hypodermis (yellow)

eyes requires the development of adapted instruments such as flexible surface coils.

Very high-resolution MR imaging has found a modest niche, however, in the pathology of the nail apparatus (38,39), showing that the technique can help to define accurately the location and limits of glomus tumours before excision.

CONCLUSION

In this review it has been shown that MR imaging of the skin is challenging because of the need for very high spatial resolution. The gradient amplitude of standard gradient coils is now sufficiently high in most commercial systems. Therefore, the main difficulty at present is to achieve a sufficient SNR, and endeavours in this area are mostly directed towards the development of very sensitive coils or coils made of flexible materials that can be adapted to curved anatomical areas, such as the face.

The second advantage of MR imaging of the skin is the possibility of measuring a large number of parameters characterizing the skin, and particularly its water properties. In addition to relaxation times, MT ratios and the ADC, other parameters could be used to study skin physiology. For example, the ability of MR imaging to detect flow in very small vessels (40,41) could provide information on skin vascularization in normal and pathologic conditions. Multiple quantum-filtered images, the contrast of which depends on the coupling of water and macromolecules (42) such as skin collagen, could provide more new information on the water status of the body's largest organ. Images of free radicals known to alter biological tissues, particularly the skin, were obtained by electron paramagnetic resonance (EPR) (43) and could possibly be applied in MR imaging of the skin with dynamic nuclear polarization.

In this paper an attempt has been made to show that the clinical usefulness of MR imaging of the skin remains to be proven. However, owing to the richness of information and anatomic details obtained with a totally non-invasive method, MR imaging provides a remarkable research tool to improve the understanding of normal and pathologic skin structure and physiology that could also have applications in the development of new therapeutic agents.

Acknowledgment

The authors thank Janet Jacobson for editorial assistance.

REFERENCES

1. Querleux B, Yassine MM, Darrasse L, Saint-Jalmes H, Sauzade M, Leveque JL. Magnetic resonance imaging of the skin, a comparison with the ultrasonic technique. *Bioeng. Skin* 1988; **4**: 1–14.
2. Hoult DI, Lauterbur PC. The sensitivity of the zeugmatographic experiment involving human samples. *J. Magn. Reson*. 1979; **34**: 425–433.
3. Bittoun J, Saint-Jalmes H, Querleux BG, Darrasse L, Jolivet O, Idy-Peretti I, Wartski M, Richard SB, Leveque JL. *In vivo* high-resolution MR imaging of the skin in a whole-body system at 1.5 T. *Radiology* 1990; **176**(2): 457–460.
4. Bittoun J, Querleux B, Jolivet O, Richard S. Microscopic imaging of the skin *in vivo* by using a high gradient intensity and a narrow bandwidth. In *Society for Magnetic Resonance/European Society for Magnetic Resonance in Medicine and Biology (SMR/ESMRMB)*. Nice, 1995.
5. Song HK, Wehrli FW, Ma JF. In vivo MR microscopy of the human skin. *Magn. Reson. Med.* 1997; **37**(2): 185–191.
6. McDonald PJ, Akhmerov A, Backhouse LJ, Pitts S. Magnetic resonance profiling of human skin in vivo using GARField magnets. *J. Pharm. Sci*. 2005; **94**(8): 1850–1860.
7. Kinsey ST, Moerland TS, McFadden L, Locke BR. Spatial resolution of transdermal water mobility using NMR microscopy. *Magn. Reson. Imaging* 1997; **15**(8): 939–947.
8. Wright AC, Song HK, Wehrli FW. *In vivo* MR microimaging with conventional radiofrequency coils cooled to 77 degrees K. *Magn. Reson. Med*. 2000; **43**(2): 163–169.
9. Darrasse L, Ginefri J-C. Perspectives with cryogenic RF probes in biomedical MRI. *Biochimie* 2003; **85**(9): 915–937.
10. Ginefri JC, Darrasse L, Crozat P. High-temperature superconducting surface coil for in vivo microimaging of the human skin. *Magn. Reson. Med*. 2001; **45**(3): 376–382.
11. Richard S, Querleux B, Bittoun J, Idy-Peretti I, Jolivet O, Cermakova E, Leveque JL. In vivo proton relaxation-times analysis of the

skin layers by magnetic-resonance-imaging. *J. Invest. Dermatol*. 1991; **97**(1): 120–125.
12. Richard S, Querleux B, Bittoun J, Jolivet O, Idy-Peretti I, Delacharriere O, Leveque JL. Characterization of the skin *in vivo* by high-resolution magnetic-resonance-imaging – water behavior and age-related effects. *J. Invest. Dermatol*. 1993; **100**(5): 705–709.
13. Song HK, Wehrli FW. Variable TE gradient and spin echo sequences for in vivo MR microscopy of short T-2 species. *Magn. Reson. Med*. 1998; **39**(2): 251–258.
14. Wolff SD, Balaban RS. Magnetization transfer contrast (MTC) and tissue water proton relaxation in vivo. *Magn. Reson. Med*. 1989; **10**(1): 135–144.
15. Mirrashed F, Sharp JC. In vivo morphological characterisation of skin by MRI micro-imaging methods. *Skin Res. Technol*. 2004; **10**(3): 149–160.
16. Lee DH, Kim JI, Lee HK. Investigation of biochemical changes in skin layers by NMR microscopy. *Skin Res. Technol*. 1998; **4**: 142–146.
17. Lovell CR, Smolenski KA, Duance VC, Light ND, Young S, Dyson M. Type I and III collagen content and fibre distribution in normal human skin during ageing. *Br. J. Dermatol*. 1987; **117**(4): 419–428.
18. Lavker RM, Zheng PS, Dong G. Aged skin: a study by light, transmission electron, and scanning electron microscopy. *J. Invest. Dermatol*. 1987; **88** (Suppl. 3): 44s–51s.
19. Querleux B, Richard S, Bittoun J, Jolivet O, Idy-Peretti I, Bazin R, Leveqve JL. *In vivo* hydration profile in skin layers by high-resolution magnetic resonance imaging. *Skin Pharmacol.* 1994; **7**(4): 210–216.
20. Franconi F, Akoka S, Guesnet J, Baret JM, Dersigny D, Breda B, Muller C, Beau P. Measurement of epidermal moisture content by magnetic resonance imaging: assessment of a hydration cream. *Br. J. Dermatol*. 1995; **132**(6): 913–917.
21. Mirrashed F, Sharp JC. In vivo quantitative analysis of the effect of hydration (immersion and Vaseline treatment) in skin layers using high-resolution MRI and magnetisation transfer contrast. *Skin Res. Technol*. 2004; **10**(1): 14–22.
22. Querleux B, Jolivet O, Bittoun J. In vivo proton magnetic resonance spectroscopy in human skin. In Skin Bioengineering. *Karger: Basel*, 1998; 12–19.
23. Wright AC, Bohning DE, Pecheny AP, Spicer KM. Magnetic resonance chemical shift microimaging of aging human skin *in vivo*: initial findings. *Skin Res. Technol*. 1998; **4**: 55–62.
24. Weis J, Ericsson A, Astrom G, Szomolanyi P, Hemmingsson A. High-resolution spectroscopic imaging of the human skin. *Magn. Reson. Imaging* 2001; **19**(2): 275–278.
25. Querleux B, Cornillon C, Jolivet O, Bittoun J. Anatomy and physiology of subcutaneous adipose tissue by *in vivo* magnetic resonance imaging and spectroscopy: relationships with sex and presence of cellulite. *Skin Res. Technol*. 2002; **8**(2): 118–124.
26. Zemtsov A, Ng TC, Xue M. Human in vivo ^{31}P spectroscopy of skin: potentially a powerful tool for noninvasive study of metabolism in a cutaneous tissue. *J. Dermatol. Surg. Oncol*. 1989; **15**(11): 1207–1211.
27. Bohning DE, Wright AC, Spicer KM. *In vivo* phosphorus spectroscopy of human skin. *Magn. Reson. Med*. 1996; **35**(2): 186–193.
28. Wright AC, Bohning DE, Spicer KM. Phosphorus metabolites in human skin and muscle obtained by phosphorus-31 magnetic resonance spectroscopy. *Skin Res. Technol*. 1997; **3**: 66–72.
29. Bohning DE, Pecheny AP, Wright AC, Spicer KM. Magnetic resonance coil for ^{31}P spectroscopy of skin over curved body surfaces. *Skin Res. Technol*. 1998; **4**: 63–70.
30. Sardon S, Sanchez-Alcazar JA, Collier SW, Lopez-Lacomba JL, Cortijo M, Ruiz-Cabello J. Effects of ethanol and dexamethasone on epidermis examined by *in vitro* ^{31}P magnetic resonance spectroscopy. *J. Pharm. Sci*. 1998; **87**(2): 249–255.
31. Querleux B. Magnetic resonance imaging and spectroscopy of skin and subcutis. *J. Cosmet. Dermatol*. 2004; **3**: 156–161.
32. Zemtsov A, Lorig R, Bergfield WF, Bailin PL, Ng TC. Magnetic resonance imaging of cutaneous melanocytic lesions. *J. Dermatol. Surg. Oncol*. 1989; **15**(8): 854–858.
33. Schwaighofer BW, Fruehwald FX, Pohl-Markl H, Neuhold A, Wicke L, Landrum WL. MRI evaluation of pigmented skin tumors. *Preliminary study. Invest. Radiol*. 1989; **24**(4): 289–293.
34. Maurer J, Knollmann FD, Schlums D, Garbe C, Vogl TJ, Bier J, Felix R. Role of high-resolution magnetic resonance imaging for differentiating melanin-containing skin tumors. *Invest. Radiol*. 1995; **30**(11): 638–643.
35. Maurer J, Schlums D, Knollmann FD, Garbe C, Vogl TJ, Bier J, Felix R. Failure of gadopentetate dimeglumine-enhanced, high-resolution magnetic resonance imaging to differentiate among melanin-containing skin tumors. *Acad. Radiol*. 1996; **3**(3): 186–191.
36. Graff BA, Benjaminsen IC, Melas EA, Brurberg KG, Rofstad EK. Changes in intratumor heterogeneity in blood perfusion in intradermal human melanoma xenografts during tumor growth assessed by DCE-MRI. *Magn. Reson. Imaging* 2005; **23**(9): 961–966.
37. Gaustad JV, Benjaminsen IC, Graff BA, Brurberg KG, Ruud EB, Rofstad EK. Intratumor heterogeneity in blood perfusion in orthotopic human melanoma xenografts assessed by dynamic contrast-enhanced magnetic resonance imaging. *J. Magn. Reson. Imaging* 2005; **21**(6): 792–800.
38. Liffers A, Vogt M, Ermert H. In vivo biomicroscopy of the skin with high-resolution magnetic resonance imaging and high frequency ultrasound. *Biomed. Tech. (Berl.)* 2003; **48**(5): 130–134.
39. Drap JL, Idy-Peretti I, Goettmann S, Wolfram-Gabel R, Dion E, Grossin M, Benacerraf R, Guerin-Surville H, Bittoun J. Subungual glomus tumors – evaluation with MR imaging. *Radiology* 1995; **195**(2): 507–515.
40. Drapé JL, Wolfram-Gabel R, Idy-Peretti I, Baran R, Goettmann S, Sick H, Guerin-Surville H, Bittoun J. The lunula: a magnetic resonance imaging approach to the subnail matrix area. *J. Invest. Dermatol*. 1996; **106**(5): 1081–1085.
41. Gens F, Remenieras JP, Patat F, Diridollou S, Berson M. Potential of a high-frequency correlation method to study skin blood flow. *Skin Res. Technol*. 2000; **6**(1): 21–26.
42. Klarhofer M, Csapo B, Balassy C, Szeles JC, Moser E. High-resolution blood flow velocity measurements in the human finger. *Magn. Reson. Med*. 2001; **45**(4): 716–719.
43. Navon G, Shinar H, Eliav U, Seo Y. Multiquantum filters and order in tissues. *NMR Biomed*. 2001; **14**(2): 112–132.
44. He GL, Samouilov A, Kuppusamy P, Zweier JL. In vivo EPR imaging of the distribution and metabolism of nitroxide radicals in human skin. *J. Magn. Reson*. 2001; **148**(1): 155–164.

DOI: 10.1002/nbm